









Copyright© Author(s) - Available online at dirjournal.org.
Content of this journal is licensed under a Creative Commons
Attribution-NonCommercial 4.0 International License.

Factors influencing diagnostic yield and complication risk in computed tomography fluoroscopy-guided lung biopsies: a 10-year single-center study

 Nabeel Mansour¹
 Hannah Gildein¹
 Frederik F. Strobl²
 Osman Öcal^{1,3}
 Tobias Geith⁴
 Daniel Pühr-Westerheide¹
 Matthias Stechele¹
 Sinan Deniz¹
 Muzaffer R. Ümütlü¹
 Nicola Fink¹
 Dirk Mehrens¹
 Moritz Wildgruber¹
 Max Seidensticker¹
 Maximilian F. Reiser¹
 Jens Ricke¹
 Philipp M. Paprottka^{4#}
 Matthias P. Fabritius^{1#}

¹LMU University Hospital, LMU Munich, Department of Radiology, Munich, Germany

²DIE RADIOLOGIE, Munich, Germany

³Heidelberg University Hospital, Department of Diagnostic and Interventional Radiology, Heidelberg, Germany

⁴University Hospital Klinikum Rechts Der Isar TUM, School of Medicine, Technical University of Munich, Department of Interventional Radiology, Munich, Germany

#Contributed equally

Corresponding author: Nabeel Mansour

E-mail: Nabeel.Mansour@med.uni-muenchen.de

Received 04 June 2025; revision requested 12 July 2025; accepted 28 July 2025.



Epub: 11.09.2025

Publication date:

DOI: 10.4274/dir.2025.253496

PURPOSE

Computed tomography fluoroscopy (CTF)-guided biopsy is an established technique for sampling pulmonary lesions, particularly with the growing prevalence of lung nodule screening programs. This study investigated procedural and lesion-related factors affecting success and complication rates in routine CTF-guided lung core-needle biopsies at a tertiary center.

METHODS

Consecutive patients undergoing percutaneous CTF-guided lung biopsies over a 10-year period (2007–2016) were retrospectively analyzed. Data collected included lesion characteristics, procedural details, and outcomes, including technical and clinical success and complications. Multivariable logistic regressions were used to identify predictors of complications and biopsy failure.

RESULTS

Among 641 patients (43% female; median age 67 years) with a median lesion size of 3.1 cm, technical and clinical success rates were 99% and 93%, respectively. Clinical success was associated with multiple pulmonary lesions and longer specimen length, with multivariable analysis identifying multiple lesions as the sole independent predictor [odds ratio (OR): 2.4]. Major complications (n = 70, 11%), primarily pneumothorax (n = 62, 90%), were associated with a longer intrapulmonary needle tract, greater pleura-to-lesion distance, smaller lesion size, fissure crossing, and the presence of emphysema or subpleural air cysts. Multivariable analysis identified smaller lesion size (OR: 0.8) and greater pleura-to-lesion distance (OR: 1.5) as independent risk factors.

CONCLUSION

CTF-guided lung biopsy is a safe and effective method for tissue sampling with high diagnostic success rates. Although multiple samples do not increase the risk of major complications, factors such as small lesion size, greater pleura-to-lesion distance, and emphysema-related changes are associated with a higher incidence of pneumothorax, emphasizing the need for risk-aware procedural planning.

CLINICAL SIGNIFICANCE

CTF-guided lung biopsy demonstrates high diagnostic performance in routine practice. Understanding how specific anatomical features influence complication risk can guide radiologists in selecting safer biopsy approaches, especially in patients undergoing evaluation through lung cancer screening programs. Integrating these risk factors into procedural planning supports more informed, patient-centered decision-making in routine clinical practice.

KEYWORDS

Biopsy, computed tomography, fluoroscopy, interventional, lung

Lung cancer remains the leading cause of cancer-related deaths worldwide, accounting for the highest mortality among both men and women.¹ Low-dose computed tomography (CT) screening has been shown to reduce mortality significantly in high-risk populations, as demonstrated by the National Lung Screening Trial and confirmed by European randomized trials.²⁻¹⁰ The widespread adoption of CT imaging, both for screening and routine diagnostics, has led to a marked increase in the detection of pulmonary nodules, including incidental findings in asymptomatic patients.¹¹⁻¹⁴

Recent advancements in imaging technology and artificial intelligence have improved the detection and characterization of these nodules. However, accurate diagnosis and timely intervention remain essential, particularly as early and minimally invasive approaches are increasingly favored.¹⁵⁻¹⁷ At the same time, the rise of precision oncology and molecular profiling has shifted clinical focus toward targeted therapies based on tumor genetics.¹⁸ This shift has increased demand for larger and repeated biopsy samples to assess histologic transformation, tumor heterogeneity, and resistance mutations.¹⁸⁻²² Evidence suggests that obtaining at least three core samples optimizes diagnostic yield, and four or more enhances the accuracy of next-generation sequencing.²³

Percutaneous transthoracic needle biopsy (PTNB) is widely used for evaluating pulmonary nodules that are inaccessible via a transbronchial route. Both CT and CT fluoroscopy (CTF) guidance are common techniques, especially for small or deep lesions.^{24,25} Among

these, CTF offers real-time imaging with continuous needle visualization, improving targeting accuracy and reducing procedure time compared with conventional stepwise CT guidance.²⁶⁻²⁸ These advantages are further supported by the radiologist's presence during the procedure, allowing immediate adjustments as needed. However, the benefits of CTF must be balanced against increased radiation exposure to both patients and operators, as well as the need for specialized training and equipment.

Despite its established safety and diagnostic performance, there remains a limited understanding of how clinical and procedural variables influence outcomes and complication rates in routine CTF-guided lung biopsies. This study aims to address this gap by evaluating a heterogeneous patient cohort, encompassing a range of needle sizes, procedural techniques, and lesion characteristics.

Methods

Patients

A retrospective analysis was conducted on all patients who underwent routine CTF-guided core-needle lung biopsies at the LMU University Hospital between 2007 and 2016. Each case had been previously reviewed by a multidisciplinary team comprising oncologists, radiation oncologists, surgeons, and interventional radiologists to assess the clinical indications in accordance with the guidelines for radiologically guided lung biopsies.²⁹ Pre-biopsy imaging, including CT, positron emission tomography/CT, or magnetic resonance imaging, was assessed to evaluate the feasibility of the transthoracic biopsy procedure. In some cases, patients had undergone previous unsuccessful histological sampling via transbronchial needle aspiration. Patients undergoing lung biopsy were initially identified retrospectively through hospital procedural scheduling and billing systems, which captured all planned and completed CTF-guided lung biopsies during the study period. Excluded cases were identified during the data curation process and were removed due to incomplete or missing key data elements, including biopsy outcome, complication documentation, or procedural imaging. These exclusions were not based on cancelled or declined biopsies but rather on documentation gaps that precluded reliable inclusion in the analysis. Informed consent was obtained at least 24 hours before the procedure, following a comprehensive explanation of the procedure and its potential complications. Pre-procedural

evaluations included serum creatinine level, platelet count, and coagulation parameters. Anticoagulation medications were discontinued before the biopsy, following the Society of Interventional Radiology (SIR) Guidelines.³⁰ All procedures in this study were conducted in accordance with the institutional ethics board of the Ludwig Maximilian University of Munich (protocol number: IRB 17-410, date: 28.06.2017) according to the Declaration of Helsinki.

Data collection

Data extracted from medical records and images included information on patient positioning, access point, the use of a coaxial technique or direct puncture, needle size, the size and location of the targeted lesion, various needle tract measurements, the presence of solitary or multiple lesions, and biopsy outcomes, including the number and length of the obtained specimens. Additionally, lung parenchymal changes, such as emphysema, air cysts, or fibrotic alterations, were retrospectively assessed on pre-procedural CT images and categorized as absent, emphysema/air cyst, or fibrosis. The density of the planned biopsy tract was also measured in Hounsfield units (HU) by averaging the attenuation at the midpoint of the needle path on non-contrast CT.

The number of pleural passes, however, was not systematically recorded and could not be reliably extracted from procedural documentation. Although the specimen count was used as a surrogate in some analyses, it does not always reflect the actual number of pleural entries. In direct puncture cases, multiple specimens may be obtained through a single pass, whereas in coaxial procedures, additional entries may occur despite a typically single-access approach. To assess procedure-associated complications, an experienced interventional radiologist with >8 years of expertise reviewed all CT images obtained during the procedures. Additionally, patient records were reviewed to document complications occurring during the procedure that were not identifiable on imaging alone or within the 30-day post-procedural period.

Biopsy procedures

All procedures were performed on multi-detector CT scanners with fluoroscopy mode, including primarily 128-slice systems (Definition Edge, Definition AS, and Flash, Siemens Healthineers, Erlangen, Germany; Optima CT660 and Discovery, GE Healthcare,

Main points

- Computed tomography fluoroscopy-guided lung biopsy is a highly effective technique, achieving a clinical success rate of 93% and technical success rate of 99% in a large, real-world cohort.
- The procedure is safe, with major complications occurring in only 11% of cases—most commonly treatable pneumothorax requiring chest tube placement.
- Small lesion size and greater pleura-to-lesion distance are the strongest predictors of complications and should be considered when planning biopsies.
- Taking multiple tissue samples does not increase complication rates.
- The presence of multiple pulmonary lesions significantly improves diagnostic success, offering flexibility in selecting the most accessible or safest target.

Waukesha, USA), which together accounted for 619 procedures. Additionally, two 16-slice systems (Sensation 16 and Emotion/Aura, Siemens Healthineers) were used in 22 procedures. Scanning parameters typically included 10–20 mAs and 120 kV. The procedures were performed by a board-certified interventional radiologist with ≥ 6 years of experience or a radiology resident in years 3–5 under the supervision of a board-certified radiologist. Operator experience was categorized based on this documentation—either as procedures performed by certified specialists or supervised residents—and used for subgroup analysis. For planning and monitoring, an online dose modulation system (CareDOSE 4D, Siemens Medical Solutions, Forchheim, Germany) was used, adjusting tube current to patient anatomy within ranges of 80–120 kV and 100–200 mAs. A non-contrast-enhanced planning CT determined the lesion's size and optimal approach. The true-cut biopsy system's diameter and length were selected based on individual lesion characteristics (13–18 gauge). These included lesion depth from the pleural surface, overall puncture length, and suspected lesion composition, such as necrosis or firmness indicative of fibrosis or malignancy, as assessed on prior imaging. A semi-automatic spring-loaded cutting needle system was used for all procedures. Patient positioning (supine, prone, or lateral) was adjusted according to the planned access trajectory. Key considerations for the needle approach included avoiding fissures, selecting the shortest path from the visceral pleura to the lesion, steering clear of ves-

sels and bronchi, and positioning the lesion dependently. Following skin disinfection, sterile draping, and the administration of local anesthesia (2% Scandicain, AstraZeneca, London, UK), a small skin incision was made. Under CTF guidance, the coaxial needle (for coaxial approaches) or the biopsy needle (for direct punctures) was intermittently advanced toward the lesion until proper positioning was achieved. Between one and five true-cut samples were collected, fixed in formalin, and sent to the pathology department for histological analysis. A post-procedure unenhanced CT was obtained to check for complications. Each needle pass through the lung parenchyma was documented with fluoroscopic images saved to the picture archiving and communication system. Patients with small, asymptomatic pneumothorax or intrapulmonary hemorrhage received conservative treatment (case example: see Figure 1). If no pneumothorax was detected on CT, patients were observed clinically for 2 hours, with radiography performed only if symptoms developed.

Technical and histopathological results

Procedures were considered technically successful if at least one histological sample of the target was obtained. Cases where tissue type, tumor grade in case of malignancy, and a definitive histopathological diagnosis of the lesion could be established were classified as clinically successful. Samples containing insufficient tissue for histologic diagnosis were documented and classified as technically successful but clinically unsuccessful.

Complications

Peri-procedural complications were classified as major or minor based on the SIR Guidelines.^{31,32} Minor complications were defined as events with no lasting sequelae, requiring minimal therapy or brief hospital observation, such as pneumothorax not requiring intervention, localized pulmonary hemorrhage (ground-glass opacity), or short episodes of hemoptysis. Major complications included events leading to hospitalization (for outpatients), unplanned escalation of care, prolonged hospitalization, permanent sequelae, or death.

Effective patient dose

For each procedure, the effective patient radiation dose was calculated. The effective dose was determined by summing the doses from the pre-procedural planning CT, all intra-procedural CT fluoroscopic acquisitions, and the post-procedural CT, as recorded in the CT examination protocol. Effective doses for the planning CT scan and post-procedural control CT scan were calculated using the formula ($E = DLP \times t$), where E is the effective dose, DLP is the dose length product, and t is the tissue weighting factor. The tissue weighting factor for the chest region was defined as $t = 0.0147$.³³ The effective dose for the sum of all CTF acquisitions was calculated using the adjusted formula for CTF ($E = DLP \times k$), with $k = 0.018 \text{ mSv} / (\text{mGy.cm})$ for chest imaging radiation. As over 95% of procedures were performed on 128-slice CT systems, dose calculations were mainly based on these systems, and data from 16-slice systems were not analyzed.

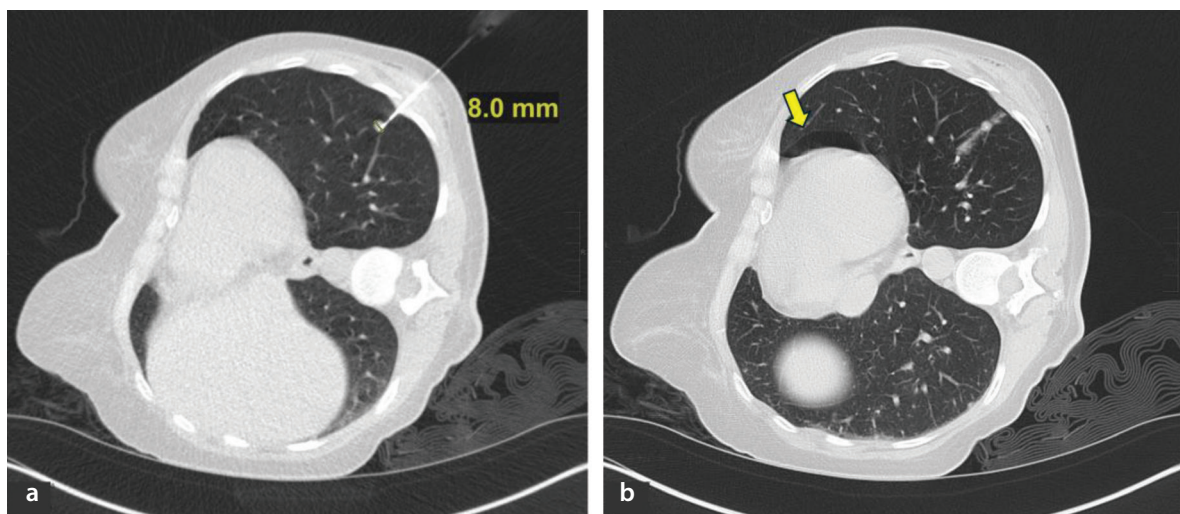


Figure 1. Computed tomography (CT) fluoroscopy-guided lung biopsy of an 8 mm nodule in the left lower lobe in a female patient with suspected recurrence of ovarian carcinoma. (a) Fluoroscopic image during the procedure, performed with the patient in the right lateral decubitus position using an 18G semi-automatic spring-loaded cutting needle system. (b) Post-procedural CT scan showing minor hemorrhage at the puncture site and a small ventral pneumothorax (yellow arrow), both of which were successfully managed conservatively.

separately due to their minimal representation.

Statistical analysis

Data analysis was performed using R software (version 4.4.1). Descriptive statistics, including medians with interquartile ranges (IQRs) and means with standard deviations, were calculated to summarize the data. The Mann–Whitney U test was applied to compare medians between two independent groups. Univariable and multivariable regression analyses were conducted to identify factors associated with clinical outcomes. Multivariable binary logistic regressions were performed, including baseline covariates with $P < 0.05$ in univariate analysis, as well as sex, age, and occasionally other variables of clinical interest, even if they did not reach statistical significance in univariate analysis. Variables not meeting these criteria (e.g., needle size for clinical success or major complication) were excluded from the respective multivariable models. In cases of collinearity, only one of the correlated variables was included in the multivariable model to ensure robustness. A P value of <0.05 was considered statistically significant.

Results

Patient characteristics

A total of 641 patients were included in the study (Table 1). Of these, 365 (57%) were male and 276 (43%) were female, with a median age of 67 years (IQR: 59–73 years). Emphysematous or cystic lung changes were present in 363 cases (56.7%), representing the predominant pattern among patients with parenchymal abnormalities, whereas fibrotic changes were observed in only 10

cases (1.6%). Patients had solitary lesions in 52.3% of cases and multiple lesions in 47.7%.

Procedural characteristics

Technical success was achieved in 638 out of 641 procedures (99%), with only three instances of technical failure. Clinical biopsy success was achieved in 593 (93%) cases. The median fluoroscopy time was 7 minutes (IQR: 4–11 minutes). General anesthesia was required in 2% of cases, and the remainder were conducted under local anesthesia. Procedures were almost evenly performed by the two groups of radiologists (53% by an attending and 47% by a resident radiologist). A total of 575 (90%) biopsies were performed using direct puncture and 66 (10%) using the coaxial technique. The overall needle tract from skin to the lesion was 7.7 cm (IQR: 6.2–9.5 cm), with a corresponding intrapulmonary needle tract length of 3.3 cm (IQR: 2.3–4.6 cm). The median shortest pleura-to-lesion distance was 0.8 cm (IQR: 0–2.1 cm). The maximal lesion diameter was 3.1 cm (IQR: 1.9–5.3 cm) and did not differ significantly between clinically successful and failed biopsies (3.22 vs. 2.57 cm, $P = 0.11$). The smallest successfully biopsied lesion measured 0.5 cm, and the largest reached 17.8 cm. Juxtapleural lesions were present in 47% of cases. The median number of specimens acquired during a procedure was 2 (range: 1–5), and the median specimen length was 14 mm (IQR: 8–24 mm). Needle size was documented in 605 procedures, with an 18G needle being the most used (491 cases, 81%), followed by a 16G needle (107 cases, 18%) and larger needles (13–14G) in a small subset (6 cases, 1%). The median total effective dose was 7.5 mSv (IQR: 5.6–10.1 mSv), with a median fluoroscopy-specific dose of 0.7 mSv (IQR: 0.4–1.2 mSv).

Pathology analysis

Histological analysis of the 593 clinically successful biopsies confirmed malignancy in 468 cases (79%). In the remaining 125 cases (21%), malignancy was excluded. Among the malignant cases, adenocarcinoma was identified in 207 cases (35%), squamous cell carcinoma in 84 cases (14%), and other tumor entities in 177 cases (30%). Technical failure occurred in 3 cases (0.5%) due to the absence of material.

Parameters influencing clinical biopsy success

The univariable analysis identified several factors significantly associated with clinical success (Table 2), including the use of coaxial technique (11% vs. 2.1%, $P = 0.049$), the presence of multiple pulmonary lesions (47% vs. 27%, $P = 0.007$), a longer specimen length (14 mm vs. 9 mm, $P = 0.013$), and a narrower angle of entry observed in the failure cohort (57° vs. 68°, $P = 0.034$). Although the acquisition of at least three specimens showed a numerical difference (27% vs. 19%), the association was not statistically significant ($P = 0.2$). In multivariable analysis, only the presence of multiple pulmonary lesions remained significantly associated with clinical biopsy success [odds ratio (OR): 2.4, 95% confidence interval (CI): 1.1–5.1, $P = 0.020$]. Lung parenchymal changes (emphysema, air cysts, or fibrosis) were not significantly associated with clinical biopsy success ($P = 0.52$, chi-squared test). Similarly, attenuation values along the puncture tract showed no significant difference between clinically successful and failed procedures (median –857.0 vs. –855.5 HU, $P = 0.77$, Wilcoxon rank-sum test).

Complications

The most common complication was pneumothorax, occurring in 227 (35%) patients, followed by superficial puncture site bleeding ($n = 46$; 7%) and mild hemothorax ($n = 7$; 1%). Less frequent complications included systemic effects of local anesthetic ($n = 1$), transient unconsciousness ($n = 1$), and pleural effusion ($n = 1$). There were no instances of air embolism in the cohort. When stratified by complication grade, 379 patients (59%) had no complications (Grade 0), whereas 192 patients (30%) experienced minor complications (Grade 1), collectively representing 571 cases (89%) with no major complications. Major complications requiring direct intervention or prolonged hospital stay (Grade 2) occurred in 70 cases (11%). The most common was pneumothorax, affecting

Table 1. Patient characteristics		
Parameter	Frequency n (%)	Median (interquartile range)
Patients	641 (100%)	
Sex		
Male	365 (57%)	
Female	276 (43%)	
Age (years)		67 (59, 73)
Clinical biopsy success	593 (93%)	
Targeted lesion size (cm)		3.1 (1.9, 5.3)
Entity		
Malignant	468 (79%)	
Non-malignant	125 (21%)	
Total effective radiation dose (mSv)		7.5 (5.6, 10.1)
Effective radiation dose from fluoroscopy (mSv)		0.7 (0.4, 1.2)

Table 2. Univariable and multivariable analyses for clinical success

Parameter	Univariate analysis			Multivariate analysis	
	Failure n = 45 ¹	Success n = 593 ¹	P value ²	P value ³	Odds ratio (95% CI)
Sex					
Male	23 (48%)	342 (58%)	0.2	0.454	0.8 (0.4–1.5)
Female	25 (52%)	251 (42%)			
Age (years)	64 (59, 69)	67 (59, 74)	0.017*	0.252	1.0 (1.0–1.0)
Targeted lesion size (cm)	2.6 (1.7, 4.7)	3.2 (1.9, 5.5)	0.11		
Number of pulmonary lesions					
Solitary	35 (73%)	313 (53%)	0.007*	0.020*	2.4 (1.1–5.1)
Multiple	13 (27%)	280 (47%)			
Lung changes					
No changes	15 (34%)	249 (42%)	0.087		
Emphysema/air cysts	28 (64%)	336 (57%)			
Fibrosis	2 (2%)	8 (1%)			
Targeted lesion location					
Apical	22 (46%)	225 (38%)	0.12		
Mid	13 (27%)	250 (42%)			
Basal	13 (27%)	118 (20%)			
Juxtapleural lesion location	23 (48%)	280 (47%)	>0.9		
Hounsfield units of puncture tract	−856 (−883, −830)	−857 (−889, −817)	0.43		
Patient positioning					
Prone	25 (52%)	284 (48%)	0.8		
Supine	15 (31%)	207 (35%)			
Side	8 (17%)	102 (17%)			
Access point					
Ventral	4 (8.3%)	90 (15%)	0.4		
Dorsal	27 (56%)	327 (55%)			
Lateral	17 (35%)	176 (30%)			
Coaxial technique	1 (2.1%)	65 (11%)	0.049		
Overall needle tract (cm)	8.4 (5.9, 9.6)	7.6 (6.2, 9.5)	>0.9		
Intrapulmonary needle tract (cm)	2.9 (1.8, 4.1)	3.3 (2.4, 4.6)	0.032*	0.523	1.1 (0.9–1.3)
Shortest pleura-to-lesion distance (cm)	1.1 (0.0, 2.3)	0.8 (0.0, 2.1)	0.5		
Angle pleura/needle (degrees)	57 (41, 78)	68 (52, 80)	0.034*	0.237	1.0 (1.0–1.0)
Fissure crossing	0 (0%)	33 (5.6%)	0.2		
Length of procedure (fluoroscopy time in minutes)	9.0 (5.5, 12.0)	7.0 (4.0, 11.0)	0.058		
Needle size (gauge)					
13	0 (0%)	3 (0.5%)	0.7		
14	0 (0%)	3 (0.5%)			
16	6 (13%)	101 (18%)			
17	0 (0%)	1 (0.2%)			
18	42 (88%)	449 (81%)			
Not documented	36	0			
Intervening radiologist					
Attending	25 (52%)	274 (47%)	0.5		
Resident	23 (48%)	308 (53%)			
Not documented	0	11			
Number of specimens					
<3	39 (81%)	432 (73%)	0.2		
≥3	9 (19%)	161 (27%)			
Overall length of biopsy specimen (mm)	9 (4, 20)	14 (8, 25)	0.013*	0.103	1.0 (1.0–1.1)
Not documented	11	89			

¹Median (interquartile range); n (%).²Wilcoxon rank sum test; Pearson's chi-squared test.³Multivariable logistic regression model.

*Indicates a P value < 0.05; CI, confidence interval.

63 (90%) patients, all of whom required chest tube placement. Two patients with bleeding into the thoracic cavity and 3 patients with parenchymal hemorrhage required a prolonged hospital stay with close monitoring but no surgical or angiographic intervention. Systemic effects of the local anesthetic were observed in 1 patient. Notably, 1 patient experienced active arterial bleeding from a peripheral left pulmonary artery, which was successfully managed with angiographic coil embolization. The resulting hemothorax was drained with two large chest tubes, which were removed after 8 days. The patient was discharged 29 days after the embolization procedure. Importantly, there were no instances of periprocedural mortality among the patients. Complication rates were compared between the two biopsy techniques; major complications occurred in 11.6% of direct puncture cases and 4.5% of coaxial cases, though this difference was not statistically significant ($P = 0.122$, chi-squared test). This analysis is limited by the substantial imbalance in group sizes, with coaxial cases comprising only approximately 10% of the cohort. Additionally, patients with emphysema or air cysts were significantly more likely to develop pneumothorax than those without lung parenchymal changes (46% vs. 20%, $P < 0.0001$, chi-squared test). The presence of fibrotic changes was infrequent and did not show a significant association with pneumothorax. Furthermore, the HU values of the biopsy tract were significantly lower in patients who developed pneumothorax than in those who did not (median -876 HU vs. -846 HU, $P < 0.0001$, Wilcoxon rank-sum test), suggesting that a less dense parenchymal trajectory may contribute to increased vulnerability to post-procedural air leaks.

Parameters associated with major complications

The analysis identified several factors significantly associated with major complications (Table 3). Univariable analysis revealed procedural factors, such as a longer intrapulmonary needle tract (3.9 cm vs. 3.2 cm, $P = 0.004$) and fissure crossing (11% vs. 4.4%, $P = 0.02$). Anatomical contributors included a greater pleura-to-lesion distance (1.8 cm vs. 0.6 cm, $P < 0.001$) and smaller lesion size (2.4 cm vs. 3.3 cm, $P < 0.001$). Multivariable analysis identified independent predictors of major complications; male sex (OR: 0.4, 95% CI: 0.2–0.7, $p = 0.002$) and smaller lesion size (OR: 0.8, 95% CI: 0.6–0.9, $P = 0.002$) were significantly associated with an elevated risk, whereas a greater pleura-to-lesion distance

further increased the likelihood of complications (OR: 1.5, 95% CI: 1.1–2.2, $P = 0.016$). Other variables, including access points and overall specimen length, were not significantly associated with major complications. Further multivariable regression analysis identified distinct risk factors for pneumothorax occurrence (Table 4): a longer intrapulmonary needle tract was significantly associated with a higher likelihood of pneumothorax (OR: 1.5, 95% CI: 1.1–1.9, $P = 0.003$), as well as biopsies involving fissure crossing (OR: 4.4, 95% CI: 1.2–16.3, $P = 0.021$). Additionally, smaller lesion size significantly increased the risk of pneumothorax, with each 1 cm increase in lesion size reducing the odds (OR: 0.7, 95% CI: 0.6–0.8, $P < 0.0001$).

Discussion

In this retrospective study of 641 patients who underwent CTF-guided lung core-needle biopsies, the complication rates were consistent with previously reported findings, with pneumothorax being the most common complication (35%).^{34–36} Most complications (89%) were minor, necessitating no additional treatment and causing no extended hospital stays. Importantly, major complications, though infrequent, were promptly managed without serious adverse outcomes, highlighting the safety of this diagnostic approach in routine clinical practice.

Prior studies have demonstrated that small lesion size is an independent risk factor for pneumothorax, with up to an 11-fold increased risk for lesions ≤ 2 cm in diameter.^{37–39} Consistent with these findings, lesion size was also a significant determinant of major complications in this study (OR: 0.8). Smaller lesions were linked to a higher incidence of complications requiring therapeutic intervention, primarily pneumothorax necessitating chest tube placement. Furthermore, several well-established risk factors for pneumothorax were confirmed in this analysis.³⁴ These include a greater pleura-to-lesion distance (OR: 1.5), a longer intrapulmonary needle tract (OR: 1.5), and fissure crossing (OR: 4.4). Pleura-to-lesion distance and intrapulmonary needle tract length are strongly interrelated, as a deeper lesion naturally results in a longer tract. Their individual statistical associations likely reflect a compounded effect of target depth on complication risk, rather than fully independent predictors. Interestingly, male sex (OR: 0.4) also emerged as a risk factor for pneumothorax in our cohort. Although the underlying reason is not entirely clear, this association may reflect underlying confounding factors. Emphyse-

ma and subpleural air cysts—both associated with increased pneumothorax risk—are more prevalent among older male patients, likely due to higher historical smoking rates. In line with this, we found a significant correlation between parenchymal fragility (i.e., emphysema/air cysts) and pneumothorax occurrence. Thus, the observed sex-based difference may reflect a greater burden of structural lung changes rather than a direct effect of sex alone. Procedural variables, such as patient positioning, access point, and pleura-to-needle angle, were analyzed. Although often constrained by anatomical feasibility, they define the procedural geometry and may indirectly influence complication risk. In our cohort, dorsal and lateral approaches were most common, reflecting a preference for minimizing tract length and avoiding fissures or major vessels. Although not always modifiable, understanding their associations with outcomes remains relevant for procedural planning. Notably, pleura-to-lesion distance and intrapulmonary needle tract length, though related, are distinct; the former represents the shortest linear distance, whereas the latter reflects the actual needle trajectory chosen by the operator. This path may be angled or extended to avoid ribs or vascular structures, even in superficially located lesions.

A strength of this study is the inclusion of a large, unselected real-world cohort encompassing all lung lesions requiring biopsy, not just those with a high suspicion of a specific malignancy. This broad inclusion enhances generalizability and reflects clinical practice more accurately than studies limited to specific entities. Notably, the use of larger biopsy needles (13–18 gauge) and the acquisition of multiple samples (≥ 3) achieved high diagnostic success rates without increasing procedural complications, demonstrating the safety and effectiveness of this approach. However, it is important to note that only three procedures each were performed using 13G and 14G needles. Upon review, these cases involved large, mainly necrotic and pleura-adjacent lesions where a higher tissue yield was clinically justified. Given the small number of cases, no statistically meaningful conclusions can be drawn regarding the safety of these large-gauge needles, and these findings should be interpreted with caution. Additionally, longer biopsy specimens significantly improved diagnostic success without elevating the risk of major complications, consistent with findings from recent studies.^{40,41} A recent large cohort study by Kim et al.⁴² ex-

Parameter	Univariate analysis		Multivariate analysis		
	No n = 571 ¹	Yes n = 70 ¹	P value ²	P value ³	Odds ratio (95% CI)
Sex			0.002*	0.002*	0.4 (0.2–0.7)
Male	313 (55%)	52 (74%)			
Female	258 (45%)	18 (26%)			
Age (years)	67 (59, 74)	68 (60, 73)	0.7	0.316	1.0 (1.0–1.0)
Targeted lesion size (cm)	3.3 (2.0, 5.5)	2.4 (1.6, 3.1)	<0.001*	0.002*	0.8 (0.6–0.9)
Number of pulmonary lesions			0.4	0.273	0.7 (0.4–1.3)
Solitary	307 (54%)	41 (59%)			
Multiple	264 (46%)	29 (41%)			
Targeted lesion location			0.6		
Apical	221 (39%)	26 (37%)			
Mid	231 (40%)	32 (46%)			
Basal	119 (21%)	12 (17%)			
Juxtapleural lesion location	292 (51%)	11 (16%)	<0.001*		
Patient positioning			0.14		
Prone	283 (50%)	26 (37%)			
Supine	193 (34%)	29 (41%)			
Side	95 (17%)	15 (21%)			
Access point			0.011		
Ventral	86 (15%)	8 (11%)			
Dorsal	324 (57%)	30 (43%)			
Lateral	161 (28%)	32 (46%)			
Coaxial technique	63 (11%)	3 (4.3%)	0.08	0.225	0.4 (0.1–1.7)
Overall needle tract (cm)	7.6 (6.2, 9.4)	8.4 (6.4, 10.0)	0.12		
Intrapulmonary needle tract (cm)	3.2 (2.3, 4.5)	3.9 (3.1, 5.4)	0.004	0.53	0.9 (0.7–1.2)
Shortest pleura-to-lesion distance (cm)	0.6 (0.0, 1.9)	1.8 (1.10, 3.0)	<0.001*	0.016*	1.5 (1.1–2.2)
Angle pleura/needle (degrees)	67 (51, 80)	62 (49, 79)	0.3		
Fissure crossing	25 (4.4%)	8 (11%)	0.02	0.064	2.9 (0.9–8.8)
Length of procedure (fluoroscopy time in minutes)	7.0 (4.0, 11.0)	7.0 (3.0, 12.0)	>0.9		
Needle size (gauge)			0.4		
13	3 (0.6%)	0 (0%)			
14	3 (0.6%)	0 (0%)			
16	100 (19%)	7 (10%)			
17	1 (0.2%)	0 (0%)			
18	428 (80%)	63 (90%)			
Not documented	36	0			
Intervening radiologist			0.8		
Attending	267 (48%)	32 (46%)			
Resident	294 (52%)	37 (54%)			
Not documented	10	1			
Number of specimens			0.3		
<3	416 (73%)	55 (79%)			
≥3	155 (27%)	15 (21%)			
Overall length of biopsy specimen (mm)	14 (8, 25)	10 (6, 17)	<0.001*	0.388	1.0 (1.0–1.0)
Not documented	94	6			

¹Median (interquartile range); n (%).

²Wilcoxon rank sum test; Pearson's chi-squared test.

³Multivariable logistic regression model

*Indicates a P value < 0.05; CI, confidence interval.

Parameter	Univariate analysis		Multivariate analysis		
	No n = 414 ¹	Yes n = 227 ¹	P value ²	P value ³	Odds ratio (95% CI)
Sex			0.3	0.156	0.7 (0.4–1.2)
Male	230 (56%)	135 (59%)			
Female	184 (44%)	92 (41%)			
Age (years)	66 (59, 73)	68 (60, 74)	0.022*	0.207	1.0 (1.0–1.0)
Targeted lesion size (cm)	3.8 (2.3, 6.1)	2.5 (1.6, 3.8)	<0.001*	<0.001*	0.7 (0.6–0.8)
Number of pulmonary lesions			0.9		
Singular	224 (54%)	124 (55%)			
Multiple	190 (46%)	103 (41%)			
Lung changes			<0.001*		
No changes	214 (52%)	54 (24%)			
Emphysema/air cysts	194 (47%)	169 (74%)			
Fibrosis	6 (1%)	4 (2%)			
Targeted lesion location			0.02*		
Apical	176 (43%)	71 (31%)			
Mid	158 (38%)	105 (46%)			
Basal	80 (19%)	51 (22%)			
Juxtapleural lesion location	256 (62%)	47 (21%)	<0.001*		
Hounsfield units of puncture tract	−846 (−880, −806)	−876 (−897, −847)	<0.001*		
Patient positioning			0.8		
Prone	201 (49%)	108 (48%)			
Supine	234 (57%)	120 (53%)			
Side	114 (28%)	79 (35%)			
Access point			0.12		
Ventral	66 (16%)	28 (12%)			
Dorsal	234 (57%)	120 (53%)			
Lateral	114 (28%)	79 (35%)			
Coaxial technique	41 (9.9%)	25 (11%)	0.7		
Overall needle tract (cm)	7.6 (6.2, 9.3)	7.9 (6.4, 9.9)	0.06		
Intrapulmonary needle tract (cm)	3.0 (2.0, 4.2)	3.8 (2.9, 5.3)	<0.001*	0.004*	1.5 (1.1–1.9)
Shortest pleura-to-lesion distance (cm)	0.0 (0.0, 1.5)	1.6 (0.7, 3.0)	<0.001*	0.153	1.2 (1.9–1.6)
Angle pleura/needle (degrees)	67 (51, 81)	67 (52, 80)	0.8		
Fissure crossing	9 (2.2%)	24 (11%)	<0.001	0.021*	4.4 (1.2–16.3)
Length of procedure (fluoroscopy time in minutes)	7.0 (4.0, 10.0)	7.0 (4.0, 11.0)	>0.9		
Needle size (gauge)			0.005*	0.823	1.1 (0.5–2.2)
13	3 (0.8%)	0 (0%)			
14	1 (0.3%)	2 (0.9%)			
16	82 (21%)	25 (12%)			
17	1 (0.3%)	0 (0%)			
18	304 (78%)	187 (87%)			
Not documented	23	13			
Intervening radiologist			0.5		
Attending	196 (48%)	103 (46%)			
Resident	209 (52%)	122 (54%)			
Not documented	9	2			
Number of specimens			0.09		
<3	295 (71%)	176 (78%)			
≥3	119 (29%)	51 (22%)			
Overall length of biopsy specimen (mm)	16 (8, 25)	12 (7, 20)	0.004*	0.17	1.0 (1.0–1.0)
Not documented	69	39			

¹Median (interquartile range); n (%)

²Wilcoxon rank sum test; Pearson's chi-squared test

³Multivariable logistic regression model

*Indicates a P value < 0.05; CI, confidence interval.

amined the feasibility of CTF-guided coaxial lung biopsies, focusing on the number of cores acquired. Their findings aligned with ours, contradicting earlier research that suggested an association between the number of coaxial cores and the risk of complications.⁴³ However, a limitation of the study by Kim et al.⁴² is the restriction of inclusion criteria to patients suspected of primary lung cancer, limiting the generalizability of findings. In contrast, our analysis evaluated multiple lesion- and procedure-related variables—including lesion multiplicity, depth, and needle trajectory—providing deeper insight into predictors of success and complications across a wide clinical spectrum.

Interestingly, the presence of multiple pulmonary lesions (OR: 2.4) was the only significant factor associated with clinical success in this study. This finding is reasonable, as the availability of multiple lesions provides the operator with the flexibility to select the most promising target, such as one that is more accessible, larger in size, or located in a safer anatomical position. This strategic choice increases the likelihood of obtaining sufficient tissue for histopathological evaluation, ultimately improving the clinical success rate of the procedure.^{44,45} Remarkably, lesion size itself had no impact on the clinical success rate of biopsies, with even lesions as small as 5 mm successfully targeted and yielding sufficient tissue for histopathological analysis. Additionally, this study provides practical data on the safety of obtaining multiple core samples and employing different needle calibers in routine clinical settings—an area that remains underreported in the current literature.

Equally noteworthy is that the experience level of the performing radiologist did not influence the complication or success rates. This finding suggests that the technique is well-standardized and relatively easy to learn, making it feasible for implementation even in smaller centers with fewer annual procedures.⁴⁶ Nonetheless, maintaining high-quality standards remains crucial to ensure optimal patient outcomes and procedural safety. Radiation exposure to both patients and operators remains a notable drawback of CTF-guided procedures compared with conventional CT-guided approaches.⁴⁷ Nevertheless, fluoroscopy accounted for <10% of the total effective radiation dose during the procedures in this study. Scanner configuration (16-slice vs. 128-slice systems) may influence dose values; given the small proportion of 16-slice cases in this study (<5%), dose calculations are mainly based on the 128-slice systems. This limitation

must be taken into account when interpreting the data. Moreover, advancements in imaging technology are likely to further decrease radiation levels in the future, particularly for procedures in anatomically high-contrast areas, such as the lungs.⁴⁸

A limitation of this analysis is its retrospective, single-center design, which is subject to inherent biases, such as selection bias, and potential inaccuracies in data extraction from medical records. Notably, hemoptysis was not documented in any of the medical records in this cohort. This likely reflects the absence of higher-grade hemoptysis events that could have influenced clinical outcomes but also underscores the limitations of retrospective data collection, where less severe complications may go underreported unless explicitly documented. Similarly, other minor complications that lacked clinical consequences may not have been captured, potentially leading to an underestimation of the overall complication rate. However, major complications requiring intervention were systematically documented through imaging and clinical records, supporting the reliability of safety outcomes. Although hemoptysis is a recognized complication, its clinical relevance appears to be limited, as demonstrated by (among others) a recent study by Kim et al.⁴² (Radiology 2024), where it occurred in 2.4% of patients (20 out of 827) without major events. In addition, the number of pleural penetrations, an intra-procedural factor known to correlate with pneumothorax risk, especially in non-coaxial techniques, was not consistently documented in procedure reports or imaging archives. This reflects another inherent limitation of retrospective data collection, particularly in earlier cases. Although specimen count was used as a surrogate in some analyses, it may not reliably reflect the number of pleural entries. Despite these limitations, this study offers valuable insights into a real-world cohort, providing practical data that enhance and complement the existing literature on CTF-guided lung biopsies.

In conclusion, this study demonstrates that CTF-guided biopsy is a reliable, effective, and safe method for diagnosing pulmonary lesions. Incorporating factors associated with major complications can improve patient selection, procedure planning, and peri-procedural monitoring, thereby enhancing patient safety. These findings are particularly relevant in the era of advanced molecular diagnostics, where obtaining multiple tissue samples is essential for guiding treatment and prognosis. Prospective studies with

standardized procedural annotation could further refine risk prediction and validate these findings in varied practice settings.

Footnotes

Conflict of interest disclosure

The authors declared no conflicts of interest.

References

1. Siegel RL, Miller KD, Wagle NS, Jemal A. Cancer statistics, 2023. *CA Cancer J Clin.* 2023;73(1):17-48. [\[CrossRef\]](#)
2. Adams SJ, Stone E, Baldwin DR, Vliegenthart R, Lee P, Fintelmann FJ. Lung cancer screening. *Lancet.* 2023;401(10374):390-408. [\[CrossRef\]](#)
3. National Lung Screening Trial Research Team; Aberle DR, Adams AM, et al. Reduced lung-cancer mortality with low-dose computed tomographic screening. *N Engl J Med.* 2011;365(5):395-409. [\[CrossRef\]](#)
4. Pinsky PF, Church TR, Izmirlian G, Kramer BS. The National Lung Screening Trial: results stratified by demographics, smoking history, and lung cancer histology. *Cancer.* 2013;119(22):3976-3983. [\[CrossRef\]](#)
5. Horeweg N, van Rosmalen J, Heuvelmans MA, et al. Lung cancer probability in patients with CT-detected pulmonary nodules: a prespecified analysis of data from the NELSON trial of low-dose CT screening. *Lancet Oncol.* 2014;15(12):1332-1341. [\[CrossRef\]](#)
6. Wille MM, Dirksen A, Ashraf H, et al. Results of the randomized Danish lung cancer screening trial with focus on high-risk profiling. *Am J Respir Crit Care Med.* 2016;193(5):542-551. [\[CrossRef\]](#)
7. Paci E, Puliti D, Pegna AL, et al. Mortality, survival and incidence rates in the ITALUNG randomised lung cancer screening trial. *Thorax.* 2017;72(9):825-831. [\[CrossRef\]](#)
8. Pastorino U, Silva M, Sestini S, et al. Prolonged lung cancer screening reduced 10-year mortality in the MILD trial: new confirmation of lung cancer screening efficacy. *Ann Oncol.* 2019;30(7):1162-1169. Erratum in: *Ann Oncol.* 2019;30(10):1672. [\[CrossRef\]](#)
9. Becker N, Motsch E, Trotter A, et al. Lung cancer mortality reduction by LDCT screening—results from the randomized German LUSI trial. *Int J Cancer.* 2020;146(6):1503-1513. [\[CrossRef\]](#)
10. de Koning HJ, van der Aalst CM, de Jong PA, et al. Reduced lung-cancer mortality with volume CT screening in a randomized trial. *N Engl J Med.* 2020;382(6):503-513. [\[CrossRef\]](#)
11. Morgan L, Choi H, Reid M, Khawaja A, Mazzone PJ. Frequency of incidental findings and subsequent evaluation in low-dose computed tomographic scans for lung cancer screening. *Ann Am Thorac Soc.* 2017;14(9):1450-1456. [\[CrossRef\]](#)

12. Jacobs PC, Mali WP, Grobbee DE, van der Graaf Y. Prevalence of incidental findings in computed tomographic screening of the chest: a systematic review. *J Comput Assist Tomogr.* 2008;32(2):214-221. [\[CrossRef\]](#)
13. Tsai EB, Chiles C, Carter BW, et al. Incidental findings on lung cancer screening: significance and management. *Semin Ultrasound CT MR.* 2018;39(3):273-281. [\[CrossRef\]](#)
14. Bach PB, Mirkin JN, Oliver TK, et al. Benefits and harms of CT screening for lung cancer: a systematic review. *JAMA.* 2012;307(22):2418-2429. [\[CrossRef\]](#)
15. Chamberlin J, Kocher MR, Waltz J, et al. Automated detection of lung nodules and coronary artery calcium using artificial intelligence on low-dose CT scans for lung cancer screening: accuracy and prognostic value. *BMC Med.* 2021;19:55. [\[CrossRef\]](#)
16. Cellina M, Cacioppa LM, Cè M, et al. Artificial intelligence in lung cancer screening: the future is now. *Cancers (Basel).* 2023;15(17):4344. [\[CrossRef\]](#)
17. Schreuder A, Scholten ET, van Ginneken B, Jacobs C. Artificial intelligence for detection and characterization of pulmonary nodules in lung cancer CT screening: ready for practice? *Transl Lung Cancer Res.* 2021;10(5):2378-2388. [\[CrossRef\]](#)
18. Folch E, Costa DB, Wright J, VanderLaan PA. Lung cancer diagnosis and staging in the minimally invasive age with increasing demands for tissue analysis. *Transl Lung Cancer Res.* 2015;4(4):392-403. [\[CrossRef\]](#)
19. Piotrowska Z, Isozaki H, Lennerz JK, et al. Landscape of acquired resistance to osimertinib in EGFR-mutant NSCLC and clinical validation of combined EGFR and RET inhibition with osimertinib and BLU-667 for acquired RET fusion. *Cancer discovery.* 2018;8(12):1529-1539. [\[CrossRef\]](#)
20. Gainor JF, Dardaei L, Yoda S, et al. Molecular mechanisms of resistance to first-and second-generation ALK inhibitors in ALK-rearranged lung cancer. *Cancer Discov.* 2016;6(10):1118-1133. [\[CrossRef\]](#)
21. Silk MT, Mikkilineni N, Silk TC, et al. Prospective evaluation of unprocessed core needle biopsy DNA and RNA yield from lung, liver, and kidney tumors: implications for cancer genomics. *Anal Cell Pathol (Amst).* 2018;2018(1):2898962. [\[CrossRef\]](#)
22. Haragan A, Field JK, Davies MPA, Escriu C, Gruver A, Gosney JR. Heterogeneity of PD-L1 expression in non-small cell lung cancer: Implications for specimen sampling in predicting treatment response. *Lung Cancer.* 2019;134:79-84. [\[CrossRef\]](#)
23. Uchimura K, Yanase K, Imabayashi T, et al. The impact of core tissues on successful next-generation sequencing analysis of specimens obtained through endobronchial ultrasound-guided transbronchial needle aspiration. *Cancers (Basel).* 2021;13(23):5879. [\[CrossRef\]](#)
24. Hiraki T, Mimura H, Gobara H, et al. CT fluoroscopy-guided biopsy of 1,000 pulmonary lesions performed with 20-gauge coaxial cutting needles: diagnostic yield and risk factors for diagnostic failure. *Chest.* 2009;136(6):1612-1617. [\[CrossRef\]](#)
25. Nakamura K, Matsumoto K, Inoue C, Matsusue E, Fujii S. Computed tomography-guided lung biopsy: a review of techniques for reducing the incidence of complications. *Interv Radiol (Higashimatsuyama).* 2021;6(3):83-92. [\[CrossRef\]](#)
26. Gianfelice D, Lepanto L, Perreault P, Chartrand-Lefebvre C, Millette PC. Value of CT fluoroscopy for percutaneous biopsy procedures. *J Vasc Interv Radiol.* 2000;11(7):879-884. [\[CrossRef\]](#)
27. Froelich JJ, Ishaque N, Regn J, Saar B, Walthers EM, Klose KJ. Guidance of percutaneous pulmonary biopsies with real-time CT fluoroscopy. *Eur J Radiol.* 2002;42(1):74-79. [\[CrossRef\]](#)
28. Kim GR, Hur J, Lee SM, et al. CT fluoroscopy-guided lung biopsy versus conventional CT-guided lung biopsy: a prospective controlled study to assess radiation doses and diagnostic performance. *Eur Radiol.* 2011;21(2):232-239. [\[CrossRef\]](#)
29. Manhire A, Charig M, Clelland C, et al. Guidelines for radiologically guided lung biopsy. *Thorax.* 2003;58(11):920-936. [\[CrossRef\]](#)
30. Patel IJ, Rahim S, Davidson JC, Hanks SE, Tam AL, Walker TG, Wilkins LR, Sarode R, Weinberg I. Society of Interventional Radiology Consensus Guidelines for the Periprocedural Management of Thrombotic and Bleeding Risk in Patients Undergoing Percutaneous Image-Guided Interventions-Part II: Recommendations: Endorsed by the Canadian Association for Interventional Radiology and the Cardiovascular and Interventional Radiological Society of Europe. *J Vasc Interv Radiol.* 2019;30(8):1168-1184. [\[CrossRef\]](#)
31. Gupta S, Wallace MJ, Cardella JF, Kundu S, Miller DL, Rose SC; Society of Interventional Radiology Standards of Practice Committee. Quality improvement guidelines for percutaneous needle biopsy. *J Vasc Interv Radiol.* 2010;21(7):969-975. [\[CrossRef\]](#)
32. Sacks D, McClenny TE, Cardella JF, Lewis CA. Society of Interventional Radiology clinical practice guidelines. *J Vasc Interv Radiol.* 2003;14(9 Pt 2):199-202. [\[CrossRef\]](#)
33. Deak PD, Smal Y, Kalender WA. Multisection CT protocols: sex-and age-specific conversion factors used to determine effective dose from dose-length product. *Radiology.* 2010;257(1):158-166. [\[CrossRef\]](#)
34. Heerink WJ, de Bock GH, de Jonge GJ, Groen HJ, Vliegenthart R, Oudkerk M. Complication rates of CT-guided transthoracic lung biopsy: meta-analysis. *Eur Radiol. Eur Radiol.* 2017;27(1):138-148. [\[CrossRef\]](#)
35. Ren Q, Zhou Y, Yan M, Zheng C, Zhou G, Xia X. Imaging-guided percutaneous transthoracic needle biopsy of nodules in the lung base: fluoroscopy CT versus cone-beam CT. *Clin Radiol.* 2022;77(5):e394-e399. [\[CrossRef\]](#)
36. Ruud EA, Stavem K, Geitung JT, Borthne A, Søyseth V, Ashraf H. Predictors of pneumothorax and chest drainage after percutaneous CT-guided lung biopsy: a prospective study. *Eur Radiol.* 2021;31(6):4243-4252. [\[CrossRef\]](#)
37. Gohari A, Haramati LB. Complications of CT scan-guided lung biopsy: lesion size and depth matter. *Chest.* 2004;126(3):666-668. [\[CrossRef\]](#)
38. Yeow KM, Tsay PK, Cheung YC, Lui KW, Pan KT, Chou AS. Factors affecting diagnostic accuracy of CT-guided coaxial cutting needle lung biopsy: retrospective analysis of 631 procedures. *J Vasc Interv Radiol.* 2003;14(5):581-588. [\[CrossRef\]](#)
39. Ozturk K, Soyul E, Gokalp G, Topal U. Risk factors of pneumothorax and chest tube placement after computed tomography-guided core needle biopsy of lung lesions: a single-centre experience with 822 biopsies. *Pol J Radiol.* 2018;83:e407-e414. [\[CrossRef\]](#)
40. Huang MD, Weng HH, Hsu SL, et al. Accuracy and complications of CT-guided pulmonary core biopsy in small nodules: a single-center experience. *Cancer Imaging.* 2019;19(1):51. [\[CrossRef\]](#)
41. Tian P, Wang Y, Li L, Zhou Y, Luo W, Li W. CT-guided transthoracic core needle biopsy for small pulmonary lesions: diagnostic performance and adequacy for molecular testing. *J Thorac Dis.* 2017;9(2):333-343. [\[CrossRef\]](#)
42. Kim CR, Sari MA, Grimaldi E, VanderLaan PA, Brook A, Brook OR. CT-guided coaxial lung biopsy: number of cores and association with complications. *Radiology.* 2024;313(2):e232168. [\[CrossRef\]](#)
43. Beck KS, Kim TJ, Lee KY, Kim YK, Kang JH, Han DH. CT-guided coaxial biopsy of malignant lung lesions: are cores from 20-gauge needle adequate for histologic diagnosis and molecular analysis? *J Thorac Dis.* 2019;11(3):753-765. [\[CrossRef\]](#)
44. Saggiante L, Biondetti P, Lanza C, et al. Computed-tomography-guided lung biopsy: a practice-oriented document on techniques and principles and a review of the literature. *Diagnostics (Basel).* 2024;14(11):1089. [\[CrossRef\]](#)
45. Borelli C, Vergara D, Simeone A, et al. CT-guided transthoracic biopsy of pulmonary lesions: diagnostic versus nondiagnostic results. *Diagnostics (Basel).* 2022;12(2):359. [\[CrossRef\]](#)
46. Schmanke KE, Zackula RE, Unruh ZA, Burdick WA, Trent JJ, Ali KM. Resident experience associated with lung biopsy outcomes: a cross-sectional study of diagnostic radiology residents. Does the Level of Training Matter? *Kans J Med.* 2020;13:235-241. [\[CrossRef\]](#)

47. Kim GR, Hur J, Lee SM, et al. CT fluoroscopy-guided lung biopsy versus conventional CT-guided lung biopsy: a prospective controlled study to assess radiation doses and diagnostic performance. *Eur Radiol.* 2011;21(2):232-239. [\[CrossRef\]](#)
48. McCollough CH, Rajiah PS. Milestones in CT: Past, present, and future. *Radiology.* 2023;309(1):e230803. [\[CrossRef\]](#)